Zonal flows, GAMs and turbulence behaviour across the L-H transition in ASDEX Upgrade

G.D.Conway[1], C.Angioni[1], F.Ryter[1], G.R.Tynan[2], P.Sauter[1], J.Vicente[3], and ASDEX Upgrade Team

[1]*MPI Plasmaphysik, Euratom-Association IPP, Garching, D-85748, Germany*

[2]*Center for Energy Research, UCSD, La Jolla, CA 92093, USA*

[3]*IPFN, Euratom Association IST, Lisbon, Portugal*

1. Introduction

A complex interaction is observed between turbulence driven $E_r \times B$ zonal flow oscillations, i.e. geodesic acoustic modes (GAMs), the mean equilibrium flow, and the edge turbulence during the low to high (L-H) plasma confinement mode transition in the ASDEX Upgrade tokamak (AUG: $R_o/a \approx 1.68/0.5$ m). While GAMs are readily observed in the tokamak L-mode edge region - and indeed are seen to grow with increasing turbulence drive (e.g. the edge pressure gradient), once it has exceeded a certain threshold - they are suppressed in the less turbulent H-mode edge [1]. Previously, below the L-H transition the turbulence moderating effect of the oscillatory zonal velocity shearing/stretching of the GAM was found to dominate over the weaker mean flow shear, particularly at low density/collisionality [2]. The roles of the GAM flow shear and mean flow shear reverse above the transition. In this paper, the analysis is extended to the higher density regime and contrasted with previous results.

2. Measurement Technique

Zonal flows and GAMs are radially localized (oscillating) $E_r \times B$ flows with an $m = n = 0$ structure and finite radial extent $k_r \neq 0$. Such flow perturbations are readily measurable with the high spatial/temporal resolution of microwave Doppler reflectometry [3]. Probing the plasma obliquely, shown schematically in fig. 1, selects via Bragg scattering a turbulence wavenumber $k_\perp = 2k_o N_\perp$, where the perpendicular refractive index $N_\perp \approx \sin\theta_o$ for low curvature reflection layers, and k_o is the microwave vacuum wavenumber [4].

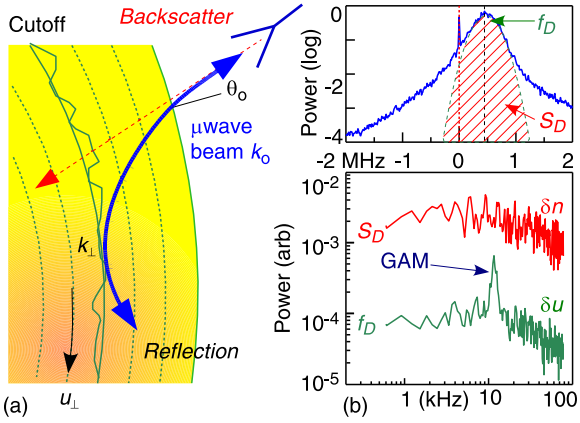

Fig. 1: (a) Schematic of Doppler reflectometer principle, (b) typical Doppler $S(f)$ and derived f_D & S_D spectra.

The backscattered reflectometer signal is Doppler frequency shifted, $f_D = u_\perp k_\perp / 2\pi$, by the perpendicular movement of the turbulence in the plasma, $u_\perp = v_{E\times B} + v_{\rm ph}$. This makes f_D directly sensitive to δE_r - cf. fig. 1(b). The backscattered signal power S_D is also a measure of δn_e at the selected $k_\perp$. Using a sliding FFT a time sequence of f_D and S_D fluctuations are generated from the weighted mean and the integral of the complex amplitude spectra $S(f)$ of the reflectometer receiver I and Q fluctuation signals [1,2,3].

3. GAM existence

Fig. 2 shows a GAM existence plot for a range of shots at various I_p and q_{95} etc. as a function of net heating power P_{net} and core line average density $\bar{n}_e$. Ohmic (green) and additionally heated L-mode (blue) GAMs are most readily observed at low n_e [2]. There are no GAMs above the L-H power threshold P_{LH} - indicated roughly by the shaded bar for the prevailing conditions in AUG with 100% tungsten coverage [5]. There is a density minimum, $\bar{n}_e \approx 4.5 \times 10^{19}\,\mathrm{m}^{-3}$, above which GAMs are generally observed only with significant heating power - partly due to the more limited access and an enhanced collisional damping. Below the low density branch of the L-H threshold are intermediate I-phase GAM discharges (purple points) with an additional limit-cycle (LC) oscillation.

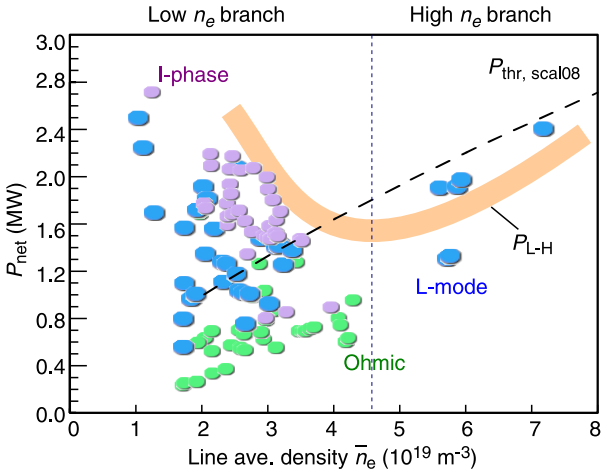

Fig. 2: GAM existence plot as a function of P_{net} and core line average density $\bar{n}_e$.

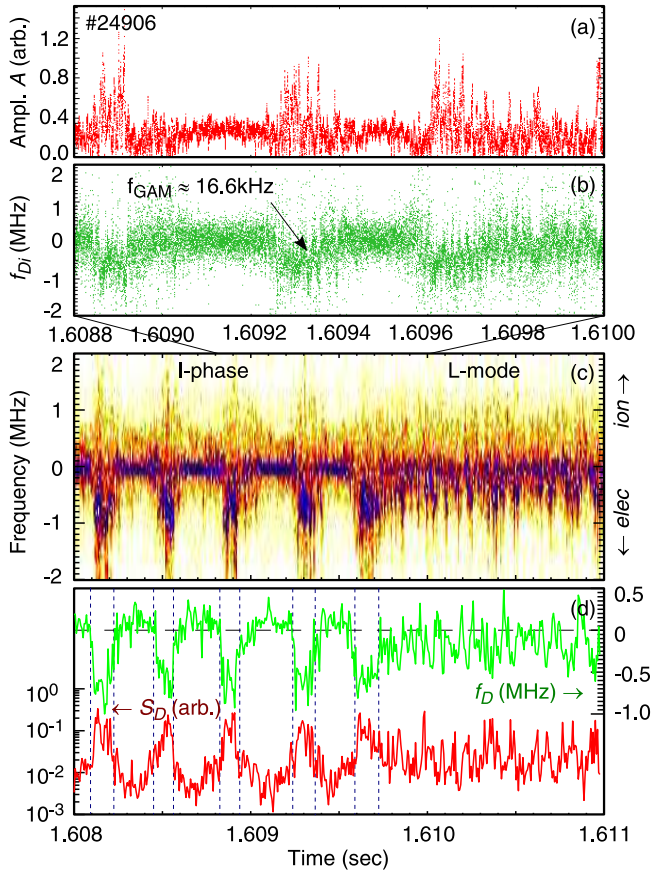

Fig. 3: Turb./flow behaviour across I-L back transition: (a) Signal A, (b) Instantaneous f_{Di}, (c) Spectrogram $S(f)$ and (d) f_D & S_D.

4. Low density GAM overview

Generally both the edge turbulence and GAM amplitude are continuous (but the GAM may show slight modulation [3]) when well away from the L-H threshold. However, for the low density branch raising either the density or net heating power sees a transition to a pulsed turbulence regime characterized by a limit-cycle behaviour sustained by competing turbulence drive and enhanced GAM flow shear suppression [2]. Similar pulsing has been observed elsewhere [6,7].

Fig. 3 shows an example of this behaviour. The middle plot is a spectrogram $S(f,t)$ of the Doppler signal from around the E_r minimum at $\rho_{pol} \sim 0.988$ across an I to L-mode back-transition. Below, are the corresponding mean f_D and S_D time traces, fig. 3(d). The temporal displacement between the cyclic growth of the turbulence and the onset of flow reversal and enhanced shearing is clearly evident. The vertical lines mark

the turbulence threshold. Within the pulse the GAM amplitude is sharply enhanced - as shown in the expanded time traces of the instantaneous Doppler frequency $f_{Di} = d\phi/dt$, where $\phi = \tan^{-1}(Q/I)$. Between the pulses the signal amplitude $A = \sqrt{I^2 + Q^2}$ is enhanced, indicating that the flow reversal is not an artifact due to loss of Doppler signal. The behaviour of gated average Doppler spectra $S(f)$ during and between the pulses also argues against a simple dithering between an L and a weak H-mode state [8].

The strong GAM inside of the E_r minimum creates an oscillatory velocity shearing rate $\tau_O^{-1} = \sigma_{u\perp}/L_r$ (where $\sigma_{u\perp}$ is the r.m.s. velocity displacement and L_r the GAM half zonal extent or radial correlation length) which tracks the (slightly smaller) turbulence decorrelation rate τ_C^{-1} measured directly from the A signal. Fig. 4 shows their evolution together with the mean flow shearing rate $\tau_M^{-1} = \Delta u_\perp/L_r$ (mean velocity step) during a slow L to H-mode transition using a neutral beam injection power ramp at low constant n_e. With increasing power the mean flow shear grows and eventually overtakes the GAM shearing, at which point the edge turbulence together with the limit-cycle activity are suppressed. The GAM is replaced by large amplitude broadband flow perturbations and clear H-mode pedestals form.

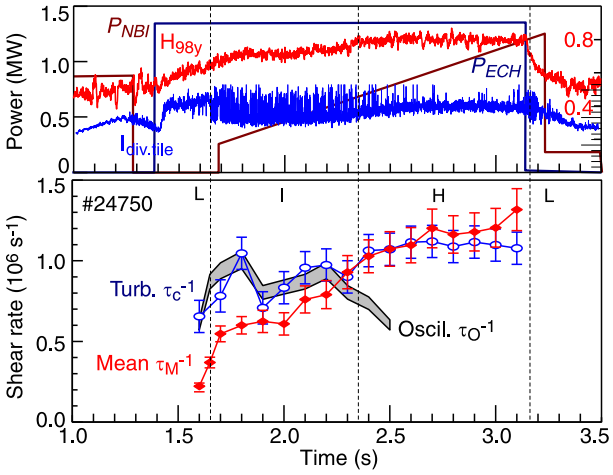

Fig. 4: Evolution of mean flow and GAM shearing rates plus turbulence decorrelation.

5. High density GAMs

With increasing density the GAM frequency f_{GAM} tends to fall, and for the high density branch the frequency drops to a few kHz is particularly pronounced. Fig. 5(a) shows f_{GAM} for a range of ohmic (green squares), L-mode (blue diamonds) and I-phase (purple triangles) discharges with varying I_p and q_{95} as a function of core line averaged density $\bar{n}_e$. Here the database is restricted to diverted plasmas with medium to large elongation since the plasma shape was previously shown to affect the GAM frequency [9]. Since the peak frequency continues to scale with the sound speed ($f_{GAM} \propto c_s$) the low frequency GAM should not be confused with a 'low frequency zonal flow'. In the I-phase discharges the limit-cycle frequency is also seen to fall with increasing $\bar{n}_e$ - due likely to zonal/collisional damping. So far, limit-cycle behaviour has not been observed in the high density branch, even for discharges close to the L-H transition.

Lower frequency GAMs might be thought to be more effective in moderating the turbulence via shearing/straining. However, the (time averaged) GAM peak-to-peak amplitude A_{GAM} (in terms of velocity perturbation [1]) also falls with the GAM frequency - as shown in fig. 5(b). On the other hand, when converting the GAM amplitude to physical displacement, A_{GAM}/ω_{GAM}, fig. 5(c), the lower frequencies can result in significantly larger (poloidal) displacements of several cm. But of course, in terms of velocity shearing rate

τ_O^{-1} the high density GAMs seem less effective. Fig. 5(d) shows the corresponding turbulence decorrelation rate τ_C^{-1} at the probing (approx. constant) $k_\perp$ value. For the low density branch there appears to be a trend of increasing decorrelation rate with $\bar{n}_e$. Here, the τ_C^{-1} follows an underlying increase in the $E \times B$ rotation (i.e. E_r well depth) and confinement. For the high density branch there appears to be a return to smaller shearing rates (data scatter excepted).

8. Discussion & Conclusions

At low n_e the GAM shearing/straining clearly plays a role in moderating the turbulence and is implicated in the H-mode transition. At higher n_e the GAM amplitude is weaker, but perhaps no less effective. Unfortunately at high n_e the current database is limited to cases with the more usual fast L-H transition associated with a sharp heating power step. This is less conducive to studying the GAM/flow evolution, such as in fig. 4. Nevertheless, even at high n_e the stronger H-mode mean flow still requires the equilibrium time scale (millisecond) to form, so there remains a potential role for the faster turbulence time scale GAM/ZF shearing to contribute to the transition. Investigations are continuing.

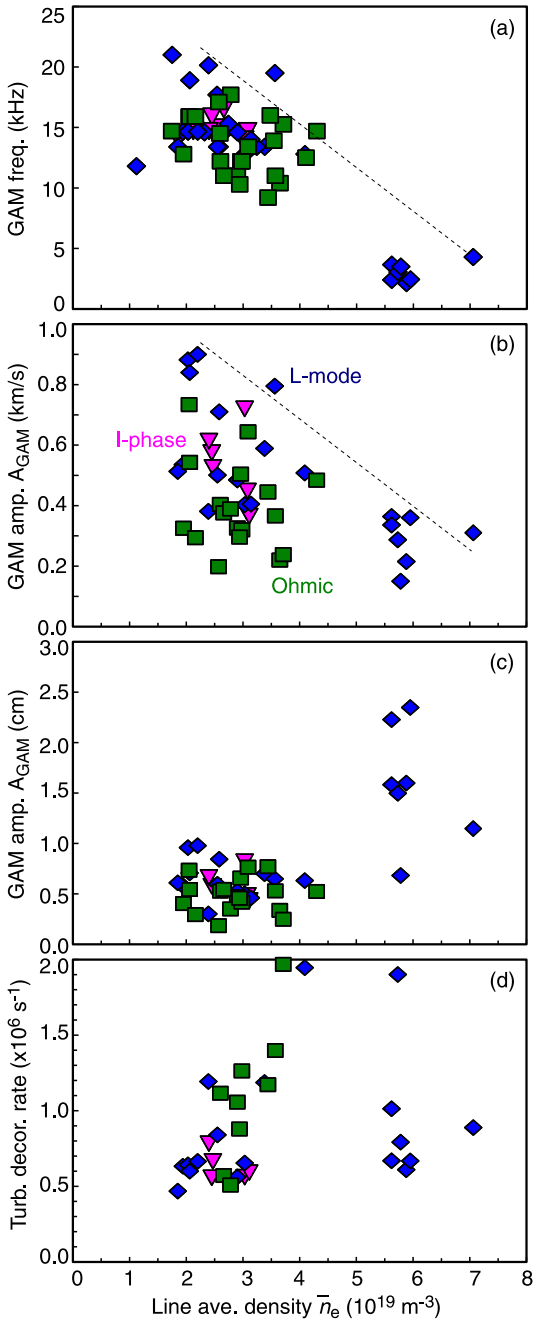

Fig. 5: (a) f_{GAM}, (b) A_{GAM}, (c) GAM p.t.p. displacement, and (d) turb. decorrelation rate τ_C^{-1} vs core line ave. $\bar{n}_e$ for various discharges.

9. References

[1] G.D.Conway *et al.* Plasma Phys. Control. Fusion **50**, 085005 (2008)

[2] G.D.Conway *et al.* Phys. Rev. Lett. **106**, 065001 (2011)

[3] G.D.Conway *et al.* Plasma Phys. Control. Fusion **47**, 1165 (2005)

[4] G.D.Conway *et al.* Plasma Fusion Res. **5**, S2005 (2010)

[5] F.Ryter *et al.* Nucl. Fusion **49**, 062003 (2009)

[6] T.Estrada *et al.* Eur. Phys. Lett. **93**, 36001 (2010)

[7] L.Schmitz *et al.* Joint EU-US Transport Task Force Workshop (San Diego), (2011)

[8] G.D.Conway *et al.* Proc. 23rd IAEA FEC (Korea) EX/7-1 (2010)

[9] G.D.Conway *et al.* Plasma Phys. Control. Fusion **50**, 055009 (2008)